The Use of an Experimental Design Approach to Investigate the Interactions of Additives used in the Making of the Negative Plate in Lead-acid Batteries

Ernst E. Ferg* and Charmelle Snyders

Department of Chemistry, Nelson Mandela Metropolitan University, P.O.Box 77000, Port Elizabeth, 6031, South Africa.

Received 28 October 2011, revised 6 September 2012, accepted 19 September 2012.

ABSTRACT

When a conventional starting, lighting and ignition (SLI) lead acid battery is exposed to a high rate partial state of charge (HRPSoC) cycling, it would experience a build-up of irreversible $PbSO_4$ on the negative plate, resulting in capacity loss and electrode damage. The addition of certain graphites to the negative paste mix has proven to be successful in reducing this effect. This study looked at using statistical design of experimental (DoE) principles to observe interactions between two graphite types and a nanocarbon together with other additives, such as $BaSO_4$ and Vanisperse, to a negative paste mixture. The response factors considered were in relation to their effect on the battery's cold cranking ability (CCA) at –18 °C, the HRPSoC and its active material utilization. Typical flooded nominal 8 Ah test cells were assembled in a reverse ratio build,with three positive and two negative plates, with three types of added carbons (flake graphite, natural graphite and nanocarbon) added to the negative paste mixture at a two-level design. The study showed the usefulness of a statistical DoE approach in the effective use of additives that are included to the negative plate paste mixture, where there are interactions between the amounts of added carbon, $BaSO_4$ and Vanisperse, with respect to the responses of CCA and HRPSoC, that do not necessarily act independently – based on their amounts – on the performance of the active material. The study also showed that there are correlations between certain response factors, such as the number of achievable cycles within a HRPSoC test sequence, and the type of added carbon.

KEYWORDS

Pb-acid battery, Pb-plate, graphite, expanders, design of experiment.

1. Introduction

The new demands made on the Pb-acid battery by automotive manufacturers and others in terms of its ability to supply extended periods of power without being fully recharged, have placed considerable strain on the battery's capabilities of providing reliable capacity performance under ahigh rate partial state of capacity (HRPSoC).[1–3] The main failure in the Pb-acid battery that was subjected to such testing criteria, was shown to be the excessive sulphation that occurred on the Pb negative plate, thereby causing irreversible cell-capacity failure.[4] Extensive work was done, in order to reduce the sulphation effect, and to improve the HRPSoC ability of a Pb-acid battery, by the addition of various types of graphites and other additives to the negative plate.[5,6] The understanding so far is that the addition of primarily conductive graphite to the negative paste mixture improves the active material's conductivity, and thereby reduces the effect of irreversible sulphation.

Also, with graphite addition, the $PbSO_4$ tends to preferentially form smaller particles dispersed throughout the active material, rather than to form larger conglomerates, thereby reducing the irreversible sulphation effect.[6] The presence of larger $PbSO_4$ crystals in the discharged active material – upon recharge – had difficulty in converting back to Pb. This,in turn, resulted in a higher current density with a higher electrode overpotential, which effectively promoted the electrolysis of water, and not necessarily the conversion of the insulating layer of $PbSO_4$ back to the Pb active material.

The addition of graphite, that was spread uniformly throughout the active material, resulted in better conductivity, and allowed for a more uniform potential gradient to exist across the material's active surface. This, in turn, lowered the overpotential of the electrode, allowing the smaller $PbSO_4$ crystals to convert more easily back to the Pb active material during the recharge step.[8]

Much work was done in varying and optimizing the amount and types of graphites, in order to extend the HRPSoC of a battery with very little being reported on the graphite's influence, and any possible interaction with the other negative plate's expander additives.[9] The use of a design of experiment (DoE) approach in the study of additives to mixtures is extensively used in the chemical industry to optimize processes and formulations.[10] These designs can often become complex, where multi-component designs are used to optimize the concentrations and indicate possible interactions between the components –to give certain desired properties.[10]

This study made use of an experimental design approach to evaluate the addition of various components (expanders) to the negative plate's paste mixture, where the extent of their interaction, dependency and independency on the cell's electrochemical properties was carefully studied. This was especially in relation to the improvement of the battery's ability to work under HRPSoC conditions. The aim of the study was not to optimize the amount of added carbon that included the graphite or other additives to a negative paste mixture, which would require several more experiments, but instead to use a two-level factorial design that would consider from a statistical point of view, the significance of varying the amounts of certain additives – or not

* To whom correspondence should be addressed. E-mail: ernst.ferg@nmmu.ac.za

Table 1 A summary of the high and low variable concentrations (weight%) for the different additives used in the statistical experimental design.

Cell number	Vanisperse/%	$BaSO_4$/%	Added carbon */%
1	0.2	0.25	1.5
2	0.2	0.25	0.5
3	0.2	0.5	1.5
4	0.2	0.5	0.5
5	0.4	0.25	1.5
6	0.4	0.25	0.5
7	0.4	0.5	1.5
8	0.4	0.5	0.5

* The added carbons were: flake graphite, natural graphite and a nanocarbon.

– on the particular electrochemical response of a Pb-acid cell, such as the cold-crank ability (CCA) and HRPSoC.

2. Experimental

2.1. Electrode Preparation and Experimental Design

The negative plates were made by following a general paste-mixing recipe and varying the added carbon (flake graphite, natural graphite and nanocarbon) concentrations with some of the other common additives, such as Vanisperse (Borregaard Vanisperse A) and $BaSO_4$ (Solvay Blanc Fixe, brilliant grade) (Table 1). The flake graphite, natural graphite and nanocarbon were supplied by Willard Batteries. A standard expander recipe used in the Pb-acid battery industry also contains a small amount of carbon black (Degussa Corax N330). In this study, carbon black, also referred to as lamp black, was included in all of the negative paste mixtures prepared, and was kept constant, at 0.15 weight%. Its role in the paste mixture is considered to contribute primarily to the formation of the active material; and it will have a lesser influence on the discharge performance and the cycle-life of the battery.

A pre-weighed amount (2.5 kg) of Barton Pot lead oxide powder (free-Pb approximately 22 % by weight) was added to a variable-speed paddle mixer, followed by the pre-weighed amounts of the additives as indicated in Table 1, which also included the lamp black at a fixed amount. Water (250 mL) was added to the mixture to form a workable paste, before the addition of sulphuric acid (SG 1.400). The acid was added at a slow rate of approximately 8 mL min^{-1} to produce a consistent homogeneous paste within approximately 10 min. Additional water was added where necessary to specific batches of the sample – to make a workable stiff paste; and the consistency thereof depended on the amount of expanders added. It was observed that the paste with a higher added-carbon content required more water, in order to obtain a workable paste. The paste density (g cm^{-3}) was measured by using an industrial standard density cup and filling it with the mixed paste to the brim of the cup.

Approximately 50 g of the active material paste was applied to one side of a 1.3 mm thick pre-cut expanded type grid (109 mm by 62 mm) made from a calcium-tin-based lead alloy. Care was taken to ensure that the paste was evenly distributed on both sides of the plate, which was then roll-pressed with a light-weight polyester non-woven material (14 gm^{-2}) on both sides of the pasted plate. The polyester material gives additional structural support to the surface of the plates during capacity-cycling applications. The pasted plates were then placed into a curing oven set at 35 °C and 85 % humidity for 48 h. The dry cured plates from a specific group of additives were subsequently formed in a bath containing sulphuric acid (SG of 1.160) for 91 h at a relatively low constant current.

Complete formation of the electrode material was confirmed by powder X-ray diffraction, thereby ensuring that less than 5 % $PbSO_4$ by weight was present in the active material. The formed plates were assembled into a five-plate design (reverse-ratio built design with three positive and two negative plates) with standard automotive polyethylene separators. The positive plates used in this study were cut from standard manufactured automotive 1.5 mm expanded grid type plates. The cells were filled with 1.280 SG sulphuric acid and subjected to a range of electrochemical tests described below.

In total, 32 cells were assembled with three variables (additives) and three responses (electrochemical tests) on which linear multiple regression tests were done to determine the significance of the low and high concentrations of the variables and their interactions to particular responses that are common to the Pb-acid battery. This was done by using ANOVA regression analysis in Microsoft Excel®.

2.2. Electrochemical Tests

The following sets of electrochemical tests (responses) were performed on a flooded five-plate cell design with an estimated theoretical capacity of about 8 Ah at the C_{20} rate (Table 2).

2.2.1. *Standard Cell Capacity and the Peukert Relationship*

The cells were capacity cycled three times at the C_{20} rate, ensuring that the cells were fully charged with little variation in the discharge capacity between the second and third discharge tests. The cells were subsequently discharged at current rates of 0.05 C_{20}, 0.10 C_{20}, 0.2 C_{20}, 0.30 C_{20}, 0.40 C_{20} and 1.0 C_{20}, respectively, followed by a standard recharge step that consisted of an 18 h charge at a voltage limit of 2.4 V, followed by a 600 mA charge of 1 h with no voltage limit. The discharge voltage limit for all tests was kept at 1.7 V; and the same recharge cycle steps were used for all of the electrochemical testing done in the study. This ensured that sufficient capacity would return to the discharged cell with a suitable upper voltage limit that would limit the water electrolysis and positive grid corrosion. The recharge capacity would vary and be dependent on the preceding discharge rate and achievable capacity. The recharge capacity would typically vary between 111 % to 116 % of the preceding discharge capacity.

Table 2 Summary of responses used in the experimental design.

Description	Responses
CCA	Time to achieve 1 V (s)
Material utilization at certain capacity rates (Ah g^{-1}/theoretical Ah g^{-1})	% Material utilization at the C_1
	% Material utilization at the C_{20}
	% Material utilization at the CCA
Peukert constants	n
HRPSoC test	Cycle number in each loop sequence

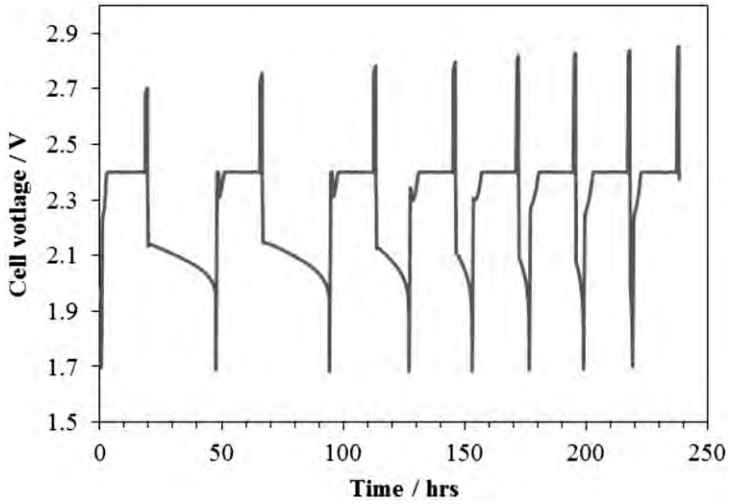

Figure 1 A typical charge and discharge profile at different current rates for cell number one made with flake graphite in the negative active material.

Table 3 Discharge and re-charge capacities of cell number one that contained flake graphite in the negative active material.

Discharge current /mA	Discharge capacity /Ah	Re-charge capacity /Ah *
400	11.19	12.65
400	11.02	12.30
800	10.83	12.16
1600	10.66	11.82
2400	10.38	11.49
3200	10.06	11.68
8000	8.05	9.19

* Includes the 0.6 Ah boost charge.

As an example, the sequential charge and discharge profile for a typical Peukert test is shown in Fig. 1. Table 3 summarizes the respective discharge capacities and the successive total re-charge capacity.

The Peukert relationship was determined by plotting the log time (t) *versus* log current (I) and from the slope of the straightline graph, the Peukert constant (n) was determined. Using the Peukert constant and the graph intercept, the respective true C_1 and C_{20} discharge capacities and currents were then determined. All capacity results were reported with respect to the negative electrode's active material, since this was the limiting component in this cell, and the material utilization was determined by using the total active material excluding the grids relative to the theoretical achievable capacity of Pb. The % capacity utilized with respect to the theoretical capacity of the weighed active material was then determined for the C_1, C_{20} and CCA rates, respectively.

2.2.2. *Cold-crank Test (CCA)*

The CCA test was done by placing the cells in a freezer for 24 h at –18 ± 1 °C prior to analysis. Since the study was comparative by nature for the size and configuration of the cells, a relationship was determined between the actual C_{20} capacity of a particular cell and the extrapolated CCA current. This was done by taking the specifications of the CCA current ratings for different battery sizes and comparing them with their respective C_{20} rated capacity. A relatively good linear relationship between the CCA current and the C_{20} rated capacity was observed for some of the international rating specifications; and the DIN European specification was chosen in this study (Fig. 2). This relationship was expressed as a

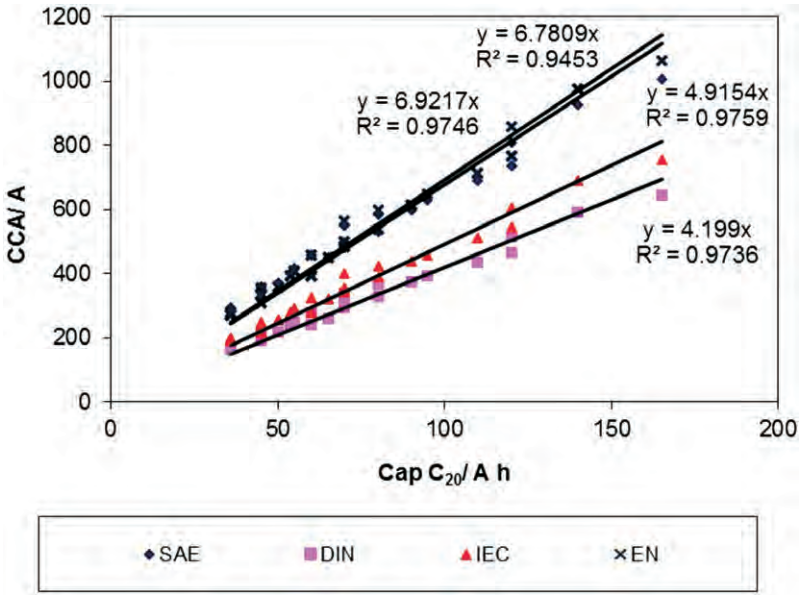

Figure 2 A comparison and relationship between the different CCA currents (A) *versus* the rated C_{20} (Ah) for a number of international accepted battery-testing specifications

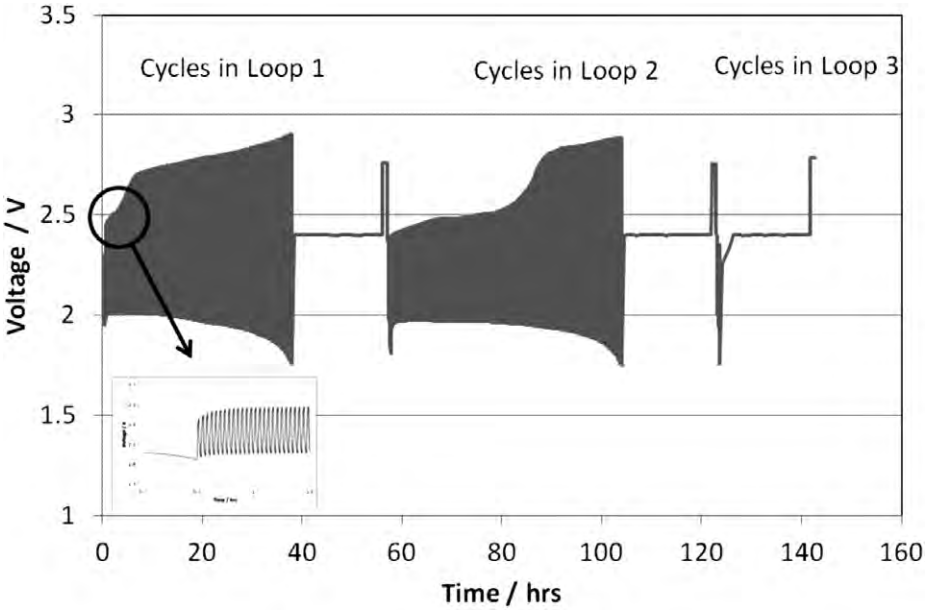

Figure 3 A typical capacity cycle sequence of a HRPSoC test at room temperature. After each loop sequence, a recharge sequence was used, followed by another cycle sequence test at partial state of charge.

straightline equation between the CCA (A) to the rated C_{20} capacity (Ah) as CCA = 4.2 C_{20}. This would allow for the comparatively high current testing of small cell designs, where the current used would depend on the actual C_{20} capacity achieved for a cell, since the C_{20} capacity for the different cells in the study could vary, due to the electrode's active material mass and density. The discharge currents ranged between 40 A and 55 A, depending on the cell's actual C_{20} capacity; and these were discharged to a lower voltage limit of 1 V, followed by a standard recharge step sequence at room temperature.

2.2.3. *High Rate Partial State of Capacity Test*

In this study, a slightly modified test sequence was used that was similar to the one described by Valenciano *et al.* [1] This required a discharge to 50 % of the actual capacity of the cell at the C_1 rate. This was followed by a one-minute charge and a one-minute discharge at the C_1 rate, respectively (Fig. 3). This sequence was repeated until the cell reached the lower discharge voltage of 1.75 V, with no upper voltage limits on the recharge step. Once this lower voltage was reached, the cell would be recharged, using the normal recharge sequence described previously that was based on the 18 h recharge at a constant voltage of 2.4 V, with a current limit of 1.8 A. The number of cycles achieved in this sequence would be described as loop sequence one. After the cell was recharged, the partial state of cycling would be repeated until the cells indicated that they were no longer able to maintain the C_1 rate of discharge to 50 %depth of discharge (DoD), or until the number of cycles within a loop count was below three cycles.

The experiment for this cell would be terminated; and the cause of the cell failure would then be determined by disassembling and analyzing the active material on the negative plate by PXRD and SEM, to determine the extent of the sulphation.

The shapes of the discharge and charge profiles between the first two loop sequences were slightly different. Notably, the end of the voltage after the recharge step and during the first sequence, quickly increased to 2.7 V, and continued to increase to 2.9 V – with a corresponding decrease in the discharge voltage until it reached the limit of 1.75 V. The cycle profile was slightly different in the second loop sequence, with the cells maintaining a relatively low recharge voltage over a large number of cycles, before climbing to 2.9 V.

In this study, none of the cells was able to achieve any significant cycle numbers (more than 3) in the third cycle sequence; and most of them showed similar charge and discharge profiles for the first and second loop sequence.

2.3. Powder X-ray Diffraction (PXRD) and Scanning Electron Microscopy (SEM)

Phase identification of a crystalline material was determined by PXRD by using a Bruker D8 diffractometer. Phase quantification was done by Rietveld refinement, using Topas V3.1. A scan range of 5–70 ° 2θ was used at 1 s/0.2 ° steps for all PXRD analysis. For the cured and formed active material taken from the plates, samples were ground by using a mortar and pestle, and the powder mounted in standard polycarbonate sample holders, before the PXRD analysis. The SEM analysis was done on a Joel JSM 6380 microscope. Samples were prepared by placing a small amount of sample onto the aluminum sample holder, using a carbon paste; and subsequently, a gold-sputter coating was applied to increase its conductivity.

3. Results and Discussion

3.1. Design of Experiment

The different electrochemical responses for the cells made with the various high and low concentrations of the additives Vanisperse, $BaSO_4$ and the different added carbon types, are summarized in Table 4. The densities of the negative plate oxide paste before application to the grid current collector are also shown.

The results were analyzed by using a linear multiple-regression model that included more than one independent variable (factor) for each response. This could be expressed in the following general format:

$$Y = b_0 + b_1\text{Vanisperse} + b_2BaSO_4 + b_3\text{Graphite} + b_4(\text{Vanisperse} \times BaSO_4) + b_5\,(\text{Vanisperse} \times \text{Graphite}) + b_6(BaSO_4 \times \text{Graphite}) + \varepsilon\,, \quad (1)$$

where Y refers to the response; b_0 is the intercept; b_1 to b_6 are the

Table 4 Summary of electrochemical responses and paste densities determined of the cells containing negative plates made with various additives and added carbon types.

Cells and graphite types		CCA time at 1 V/s	Peukert const. (n)	Material utilization at rates			HRPSoCCC		Paste density/g cm^{-3}
				CCA/%	C1/%	C20/%	Loop1/cycles	Loop 2/cycles	
Flake	1	148.8	1.129	10.90	46.83	62.70	5729	6272	4.41
	2	146.3	1.138	10.42	44.86	61.20	7390	5553	4.45
	3	125.9	1.106	9.25	49.39	62.92	2330	2090	4.01
	4	121.0	1.139	8.75	44.88	62.01	3276	2996	4.22
	5	120.3	1.149	8.63	44.45	61.66	883	1175	4.10
	6	119.8	1.158	8.76	43.96	62.62	1630	2206	4.29
	7	132.7	1.117	9.83	48.50	63.35	299	131	4.13
	8	137.0	1.116	9.60	45.83	60.09	277	334	4.32
Nat	1	137.5	1.108	9.29	45.64	57.90	1578	2036	3.92
	2	145.0	1.112	10.44	48.19	61.73	3567	3539	4.43
	3	227.1	1.179	13.40	50.60	54.16	1677	1377	3.87
	4	207.7	1.197	9.27	38.26	42.88	2569	3230	4.29
	5	142.0	1.095	9.62	47.29	58.08	552	534	3.83
	6	204.7	1.094	13.94	47.98	58.39	289	411	4.23
	7	172.6	1.082	11.29	47.02	56.06	286	295	3.88
	8	152.6	1.060	10.38	51.02	58.34	194	356	4.18
Ncarb	1	132.1	1.148	10.21	48.46	66.25	9443	5944	3.06
	2	119.6	1.201	8.98	43.70	64.38	1209	7010	3.48
	3	63.6	1.272	4.68	40.92	63.15	5222	1263	2.95
	4	62.0	1.347	4.23	34.35	58.45	7498	2570	3.73
	5	88.2	1.258	5.43	35.22	52.83	2857	1173	2.85
	6	106.9	1.168	8.22	47.34	65.95	4938	8311	3.50
	7	99.3	1.109	7.39	52.17	63.81	1280	1119	2.89
	8	144.4	1.123	11.08	50.71	65.78	6455	4436	3.49

estimated coefficients for the variables and their interactions; and ε is the experimental error.

The null hypothesis (H_o) concerning a specific coefficient b_n is usually stated as H_o:$b_n = 0$. This hypothesis (H_o) states that there is no influence of the variables (graphite, Vanisperse and $BaSO_4$) on the particular electrochemical response. A test was done to determine whether the estimated coefficient was significantly different from zero. This testing was done by making use of statistical P-values. Based on the P-value obtained from the regression analysis,the null hypothesis was then either accepted or rejected. If a high P-value (above 0.05) was obtained, H_o was accepted and it was confirmed that the values for the coefficients b_n (n = 0 to 6) could be considered as experimental noise and equal to zero. For a low P-value (below 0.05), H_o was rejected; and it could be accepted that the respective values for b_n (n = 0 to 6) were not noise; and that the particular variable and/or their interactions had had a significant effect on the response.

By a process of elimination, the variables and/or the respective interactions that had a high P-value could be excluded in subsequent regression analysis, thereby giving a better refinement of the remaining data to be reconsidered in terms of the same H_o.

As an example, the regression analysis for the response factor CCA, the time in seconds to discharge to 1 V for the cells made with the flake graphite,are shown in Table 5.

The example shows that the variables of Vanisperse and $BaSO_4$ – and their interactions were significant on the electrochemical response of CCA discharge time. A P-value of 0.05 was obtained for the Vanisperse-$BaSO_4$ interaction, but it showed a large P-value for the variable of flake graphite, and its possible interaction with the other variables in the electrode material, implying that the change in the flake graphite amount had no significant influence on this particular response.

Notably, once the interactions with a large P-value were removed from the statistical regression analysis, the respective P-values of the relevant variables and their interactions improved considerably, where a value of 0.002 was obtained, thereby showing that there was significant interaction between the Vanisperse and $BaSO_4$ concentrations, irrespective of the flake graphite amount. However, the variable of flake graphite in the final analysis, even with a high P-value, was not removed from the statistical regression analysis, since it was still present in the cell's chemical make-up. This shows that with regard to this particular response, changing the flake graphite amounts from 0.5 % by weight to 1.5 % by weight had no effect on the achievable CCA discharge time (in s) for this particular set of cells made. The determined coefficients in the final analysis give an indication of whether the change in the variable amounts have a positive or negative effect on the particular response. Interestingly, in this analysis, the coefficients for both the Vanisperse and $BaSO_4$ were negative, but their interaction was positive, implying that both are important in the active material – to give a positive increased response for the cell to discharge under CCA conditions.

This can be represented graphically by taking the calculated coefficients into consideration within the limits of the design, where the effects of changing the variable (Vanisperse and $BaSO_4$) concentrations and their interaction have on the CCA response, in terms of the time taken to discharge to 1 V (Figs 4 and 5).

For the cells made with nanocarbon, even though the P-value for Vanisperse was 0.06, a good approximation could be achieved by remembering that the model is not ideally refined, since the coefficients of the nanocarbon with a high P-value were kept in the final subsequent refinements (Table 6).

The most suitable combination of Vanisperse and $BaSO_4$ was for both of them to have the lower concentration within the

Table 5 Regression analysis for the CCA response factor with the variables $BaSO_4$, Vanisperse and flake graphite.

Refinement matrix for one response

Vanisperse (A)	$BaSO_4$ (B)	Graphite (C)	AB	BC	AC	Response CCA/s
0.2	0.25	1.5	0.05	0.375	0.3	149
0.2	0.25	0.5	0.05	0.125	0.1	146
0.2	0.5	1.5	0.1	0.75	0.3	126
0.2	0.5	0.5	0.1	0.25	0.1	121
0.4	0.5	1.5	0.2	0.75	0.6	133
0.4	0.5	0.5	0.2	0.25	0.2	137
0.4	0.25	1.5	0.1	0.375	0.6	120
0.4	0.25	0.5	0.1	0.125	0.2	120

Initial regression refinement

	Coefficients	Standard error	t-statistic	P-value
Intercept	226.5	9.95	22.764	0.027948
Vanisperse	–302.5	28.06	–10.78	0.058890
$BaSO_4$	–248	22.45	–11.05	0.057473
Graphite	11.5	6.54	1.759	0.329116
Vanisperse-$BaSO_4$	780	60	13	0.048875
$BaSO_4$-graphite	–4	12	–0.333	0.795167
Vanisperse-graphite	–30	15	–2	0.295167

Final regression refinement

	Coefficients	Standard error	t-statistic	P-value
Intercept	237	9.98	23.740	0.000164
Vanisperse	–332.5	30.95	–10.74	0.001726
$BaSO_4$	–252	24.77	–10.17	0.002023
Graphite	1	1.957	0.510	0.6447
Vanisperse-$BaSO_4$	780	78.32	9.96	0.002154

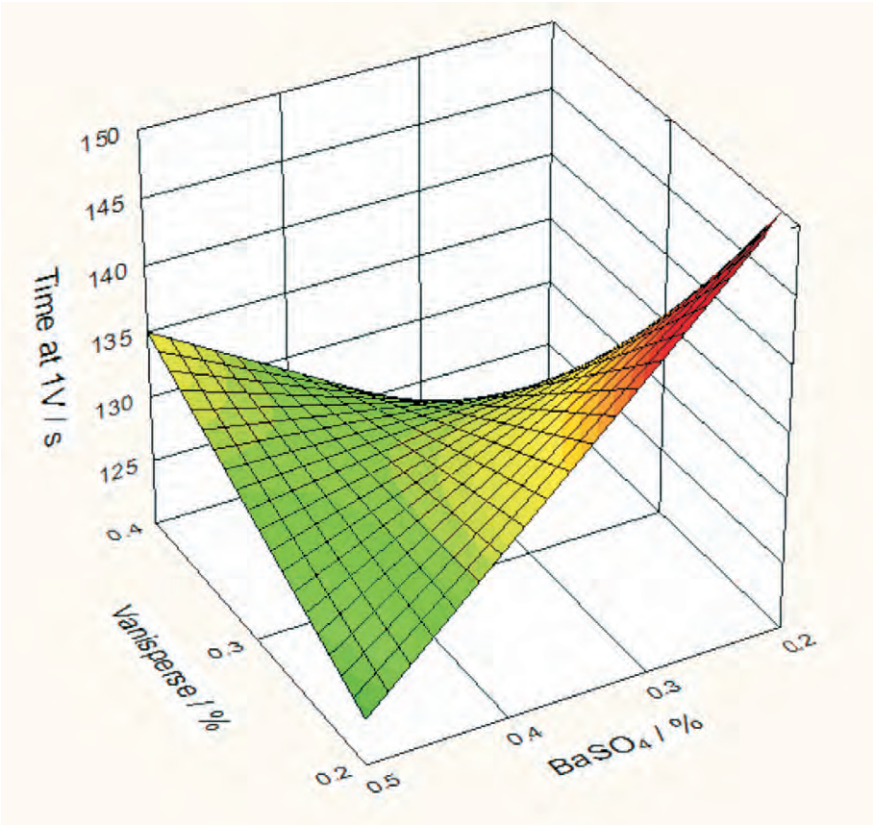

Figure 4 3D-graph of the interaction effect of the Vanisperse and $BaSO_4$ with respect to the CCA discharge time (s) for the cells made with flake graphite added to the negative active material.

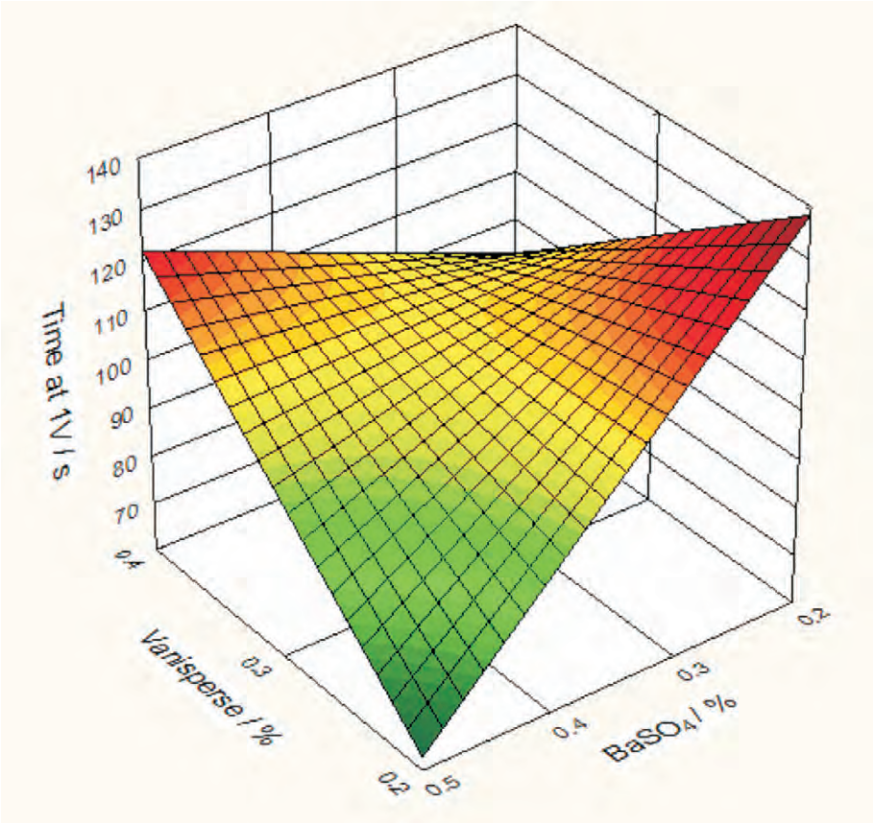

Figure 5 3D-graph of the interaction effect of the Vanisperse and $BaSO_4$ with respect to the CCA discharge time (s) for the cells made with nanocarbon added to the negative active material.

design. For the sake of completeness, the added carbons were still present in the chemical make-up of the cell, even though statistically, the null hypothesis was true,in that its influence on the response was primarily noise and equal to zero. Note that these results do not suggest an optimized concentration of the additives, but rather show that there is a trend, and more importantly, an interaction between the amounts of $BaSO_4$ and Vanisperse, respectively.

For each of the added carbon types studied, the influence of changing the Vanisperse, $BaSO_4$ and the added carbon concentrations – and their possible interactions to a particular response – are summarized in Table 6. The respective coefficients of the variables and their P-values for the particular response are shown, bearing in mind that even if the variable (added carbon) would show a large P-value, it was not excluded, since it still formed part of the cell's composition. Better statistical results could be obtained by excluding the added-carbon variable from further refinements. However, the aim of the study was not to optimize the amount of additives in the active material to a particular response, but rather to consider if there was a significant influence and possible interaction with the other additives in a two-level design.

The effect of the interaction between the Vanisperse and $BaSO_4$ that was observed for the flake graphite and nanocarbon on the CCA discharge time was not observed for the cells made with natural graphite. The average discharge times for the respective CCA tests were slightly higher when compared with the cells made with the nanocarbon and the flake graphite (Table 4). This can also be seen in the % efficiency determined at the CCA rate, where the cells with the natural graphite had on average higher values than the corresponding cells with nanocarbon and flake graphite.

There could be a number of reasons for this effect, where the cells with the natural graphite had a slightly higher average paste density than that from which the electrodes were made (Table 4). The study did not consider other influences that could play a role in the one with added carbon, to perform better than the other for a particular response. Factors, such as paste density, active surface area, porosity and metal impurities can influence the overall performance of the electrodes, especially at the low temperature and high currents employed.

The study considered only the possible influences of varying the additives to the response within the limits of the experiment. The study did show that because of the observed interaction,which showed a positive correlation, that both additives should be present in the negative plate, in order to get an increased positive response.

The study examined the effect of changing the additive amounts of Vansiperse, $BaSO_4$ and the various graphite types on the Peukert constant (n). The constant may be considered as an indication of the expected change in the capacity of a particular cell design with change in the discharge rate.[11] The results showed that there was a correlation for the cells made with the natural graphite and the interaction of the Vanisperse and $BaSO_4$ on the Peukert constant (n). Relatively low P-values were observed for the corresponding coefficients (Table 6).

This effect was, however, not observed for the cells made with the flake graphite. The results are unusual in showing the influence of additives on the Peukert constant. Most of the literature showed little or no variation in the constant for the samples made with different additives; and the small variations observed were seen as acceptable within experimental error.[11, 12] However, the results of this study showed that the slight variations of the (n) constant observed for cells with different amounts of the additives are not necessarily due to experimental error, whereupon statistical analysis the null hypothesis would have to be

Table 6 Summary of the coefficients and statistical P-values obtained from the regression analysis for the Vanisperse, $BaSO_4$ and the three carbon-type additives to the various electrochemical responses.

Flake graphite		Intercept	Vanisperse	$BaSO_4$	Graphite	Vanisperse-$BaSO_4$	Vanisperse-graphite	$BaSO_4$-graphite
CCA/s	Coefficients	237	–332.5	–252	1	780		
	P-value	0.00016	0.00173	0.00202	0.6447	0.00215		
Peukert (n)	Coefficients	1.170	0.035	0.056	–0.0125			
	P-value	7.02×10^{-7}	0.4812	0.564	0.2382			
Loop1/cycles	Coefficients	21765	–45160	–29146	–33585	55760	4705	2968
	P-value	0.00262	0.00356	0.00441	0.0112	0.00617	0.0183	0.0232
Loop2/cycles	Coefficients	11469	–16331	–9655	–355			
	P-value	0.00126	0.00524	0.0150	0.580			
% Utill CCA	Coefficients	16.693	–23.198	–17.353	0.2657	53.549		
	P-value	0.00197	0.00212	0.00259	0.168	0.00278		
% Utill C_1	Coefficients	41.693	–4.0128	8.5082	2.4081			
	P-value	3.13×10^{-5}	0.3904	0.0633	0.0447			
% Utill C_{20}	Coefficients	61.240	–1.386	0.179	1.177			
	P-value	5.39×10^{-6}	0.742	0.957	0.209			
Natural graphite		Intercept	Vanisperse	$BaSO_4$	Graphite	Vanisperse-$BaSO_4$	Vanisperse-graphite	$BaSO_4$-graphite
CCA/s	Coefficients	149.3	–56.75	130.8	–7.7			
	P-value	0.0861	0.7007	0.2998	0.793			
Peukert (n)	Coefficients	0.945	0.431	0.719	0.0003	–2.034		
	P-value	3.05×10^{-5}	0.0456	0.00626	0.973	0.0083		
Loop1/cycles	Coefficients	5469	–10088	–1260	–632			
	P-value	0.0074	0.0114	0.527	0.237			
Loop2/cycles	Coefficients	5989	–10733	–1262	–824			
	P-value	0.00480	0.00824	0.5139	0.1353			
% Utill CCA	Coefficients	7.236	37.72	–5.44	–3.19	–48.44	–16.00	21.03
	P-value	0.00777	0.00420	0.0233	0.0166	0.00699	0.00530	0.00322
% Utill C_1	Coefficients	42.069	9.00	1.21	2.20			
	P-value	0.0126	0.682	0.944	0.618			
% Utill C_{20}	Coefficients	59.85	19.67	–26.16	–0.185			
	P-value	0.00162	0.298	0.118	0.958			
Natural graphite		Intercept	Vanisperse	$BaSO_4$	Graphite	Vanisperse-$BaSO_4$	Vanisperse-graphite	$BaSO_4$-graphite
CCA/s	Coefficients	317.0	–578.3	–601.6	–12.43	1747		
	P-value	0.0162	0.0631	0.033	0.399	0.0410		
Peukert (n)	Coefficients	0.782	1.353	1.468	–0.013	–4.640		
	P-value	0.0247	0.1013	0.0504	0.7458	0.0504		
Loop1/cycles	Coefficients	7375	–9803	2008	–325			
	P-value	0.296	0.486	0.854	0.905			
Loop2/cycles	Coefficients	12735	–2185	–13050	–3207			
	P-value	0.0183	0.767	0.0771	0.0805			
% Utill CCA	Coefficients	18.87	–31.15	–47.40	6.17	–3.34	150.90	–20.40
	P-value	0.0073	0.0125	0.0066	0.0147	0.0498	0.0055	0.0102
% Utill C_1	Coefficients	35.90	22.52	3.43	0.168			
	P-value	0.0648	0.489	0.892	0.979			
% Utill C_{20}	Coefficients	65.48	–4.82	1.78	–2.13			
	P-value	0.003	0.830	0.921	0.638			

rejected due to the low P-value, and that the variables do have an influence on the particular response (n).

This showed that the amount of the additives that were added to the negative electrode could influence the discharge ability of the cell – especially at higher currents. By comparison, the cells made with the nanocarbon showed only slight effects and interaction with the Vanisperse and $BaSO_4$. In typical cells, or battery applications, there would be a desire to have an n value close to one. This would indicate that the cell or battery would have little deviation in its respective discharge capacities at different discharge rates.

In terms of the influence or effect of the additives on the number of achievable cycles in the HRPSoC response, the results showed that varying the amounts of the additives, especially the natural graphite and nanocarbon, had no effect on the number of achievable cycles in both loop sequences 1 and 2. For the cells made with the natural graphite, the results did show a reasonably small P-value for the addition of the Vanisperse with a negative coefficient. However, this was not observed for the number of cycles achieved in the second loop sequence.

For the cells made with the flake graphite, the P-values were all significantly small for all the variables and their interactions. This implies that the corresponding coefficients are significant, and that the null hypothesis could be rejected. Noticeably, there were even some significant correlations between the additives in the second loop sequence, where the results showed that the addition of Vanisperse had a significant influence on the number of achievable cycles within a loop sequence in the HRPSoC testing.

By considering the coefficient of the Vanisperse in both the natural and flake graphites, the number of cycles within the cycle testing decreased with an increase in the Vanisperse concentration. On the other hand, varying the amount of $BaSO_4$ and graphite types did not have any effect on the cells made with the natural graphite.They did still have an influence on the cells made with the flake graphite, even within the second loop sequence of the cycling test. It must, however, be remembered that the results only show that the amount of graphite does not significantly influence the number of achievable cycles within the concentration range of the experiment. Hence, this supports the idea that a certain minimum amount of the graphite in the paste mixture is sufficient to improve the cycle life, and that more graphite would not necessarily improve or achieve more capacity cycles. However, the results do indicate that the Vanisperse amount in the paste mixture could influence the number of achievable cycles.

The addition of the nanocarbon did not influence the number of achievable cycles in the HRPSoC test, and the coefficients observed could be considered as statistical noise, and that the initial null hypothesis was true. The results show that the nanocarbon within the paste mixture behaved and influenced the cell electrochemistry significantly differently when comparedwith the addition of flake or natural graphite. This could be related to differences in the particle size, surface areas and crystallinity of the various graphites, when compared with each other and the nanocarbon.

When considering the effect of new additives to the negative plate active material, its influence and possible interaction with existing additives and their effect on the cell electrochemical properties should be taken into consideration. The study showed that the amount of Vanisperse had a significant influence on some of the more common electrochemical properties in Pb-acid cells, such as CCA, and the ability to render capacity cycles at a partial state of capacity (Table 6). The results showed that the addition of various additives to improve a certain electrochemical property in a Pb-acid battery does not necessarily work in isolation, and that there was a dependency on the properties of the other additives already present.

The results also show that by using an added carbon with considerably different chemical and physical properties – to other types of carbon – certain electrochemical properties could be influenced differently. For example, the use of natural or flake crystalline graphite in comparison with the use of an amorphous nanocarbon indicated a different interaction with the other additives already present. The addition of such added carbons at the laboratory scale to a paste mixture also showed that care should be taken when adding such compounds on the larger manufacturing scale. This was particularly observed in the change in paste density, as the amount of nanocarbon was increased. Additional water had to be added to the oxide mixture, in order to maintain a workable paste. The idea that 'more is better' is not always feasible, since in this study, it was shown that for a number of electrochemical properties, the increased amount of graphite or nanocarbon did not significantly influence the response, as expected, and that the observed changes in the response could be due to the changes in the amounts of other additives, such as Vanisperse and $BaSO_4$.

The results showed that the variation in the amounts within the limits of the experiment of all three variables had no influence on the material utilization at the C_1 and C_{20} discharge rates (Table 6). The material utilizations were relatively similar at these rates, and showed that varying the Vanisperse, $BaSO_4$ and graphite amounts did not significantly influence the discharge ability, and that the null hypothesis may be accepted as valid.

The study showed that by using a design with an experimental approach to study the variation of a number of additives within certain limits, and determining their effect on a number of responses, insight into the benefit of additives – or not – on certain electrochemical properties, may be determined relatively quickly. The study showed that one does not have to consider the effect of one additive at a time, and that interactions with other additives already present in the paste mixture can occur. This also eliminates the important influence of preconceived ideas, where the increase of a certain additive amount does not necessarily improve the particular property,since the interaction can be skewedby interactions with other additives.

The two-level factorial design can now be taken further to a multi-level design,by considering only the variables that have been shown to be significant with positive interactions. These can then be designed in such a way as to optimize the amounts for a particular optimum response. However, one must also keep in mind that the benefit for one particular response can have a negative effect on another. Hence, this study showed that a minimum amount of added carbon is required, and that additives, such as the Vanisperse and $BaSO_4$ can be varied to optimize the CCA and HRPSoC responses.

The interactions and influences of the most common additives – in particular $BaSO_4$ and Vanisperse in the negative plate paste mixture on the Pb-acid cell's ability to capacity cycle – have been reported elsewhere.[12] The study also showed that different types of carbons, especially nanocarbon with the benefits of high surface area, can result in slightly different effects on certain responses, and that the optimization has to be independently confirmed by their own set of experiments.

3.2. Correlations Between the Responses for Cells made with Different Graphites

The results of the study also showed that there were possible

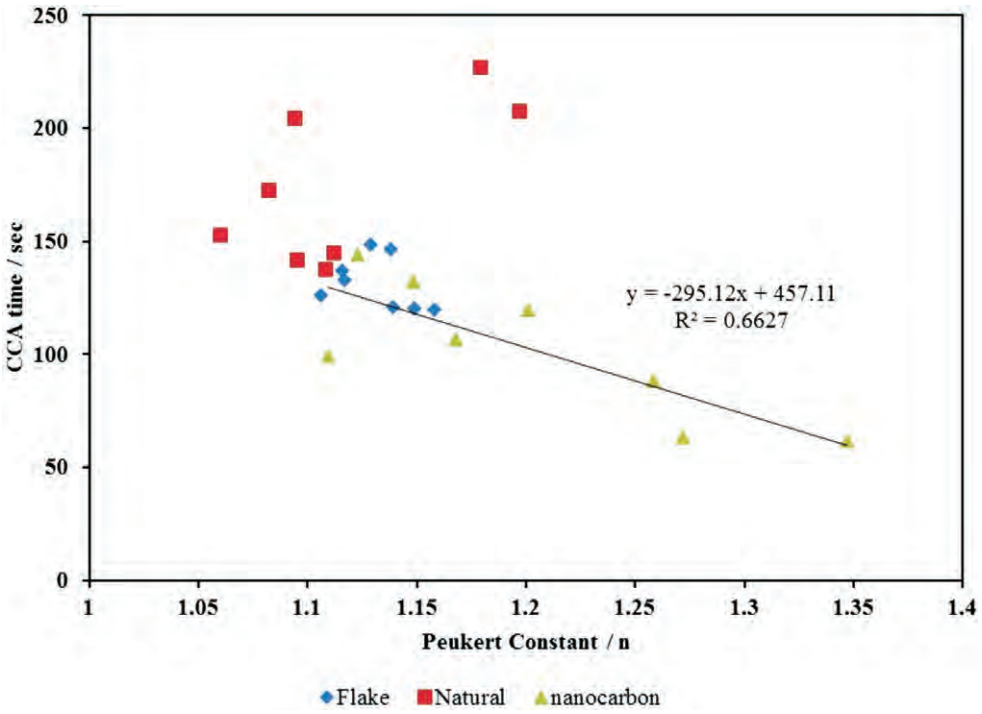

Figure 6 Correlation results between CCA discharge time and the Peukert constant for the three added carbons studied.

correlations between the different electrochemical responses of the cells that had negative plates containing different types of added carbon. Linear stepwise regressions that were done between the various responses and their respective R^2 values indicated whether there were suitable correlations, or not (Figs 6–8).

A strong correlation was observed between the response of the CCA discharge ability and the Peukert constant (n) for the cells made with the nanocarbon (Fig. 6). However, this was not observed for the cells made with the flake or natural graphite. The larger the n value, the lower the expected discharge capacity at the higher rates. These values were observed indirectly for the cell's ability to achieve lower discharge times at the CCA rates. This effect on the Peukert constant can also be seen in the results of the material used for the cells that were discharged at the C_1 rate (Fig. 7).

There were relatively poor correlations for the cells made with the flake and natural graphites for this particular response, respectively. This effect was not as prominent when comparing the material utilization at the C_{20} rate *vs* the Peukert constant.

Good correlations of 0.95 and 0.92 were observed with a gradient close to one for the comparison of the number of cycles achieved in the first and second loop sequences for cells that contained the flake and natural graphites (Fig. 8). This implied

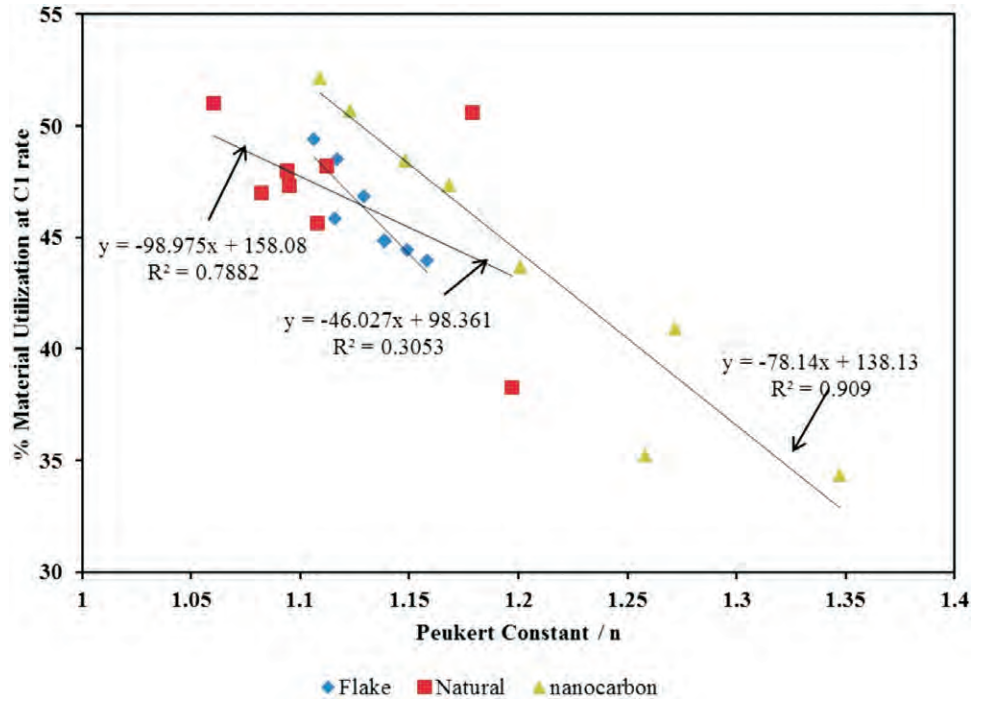

Figure 7 Correlation results between material utilization at the C_1 rate and the Peukert constant for the three added carbons studied.

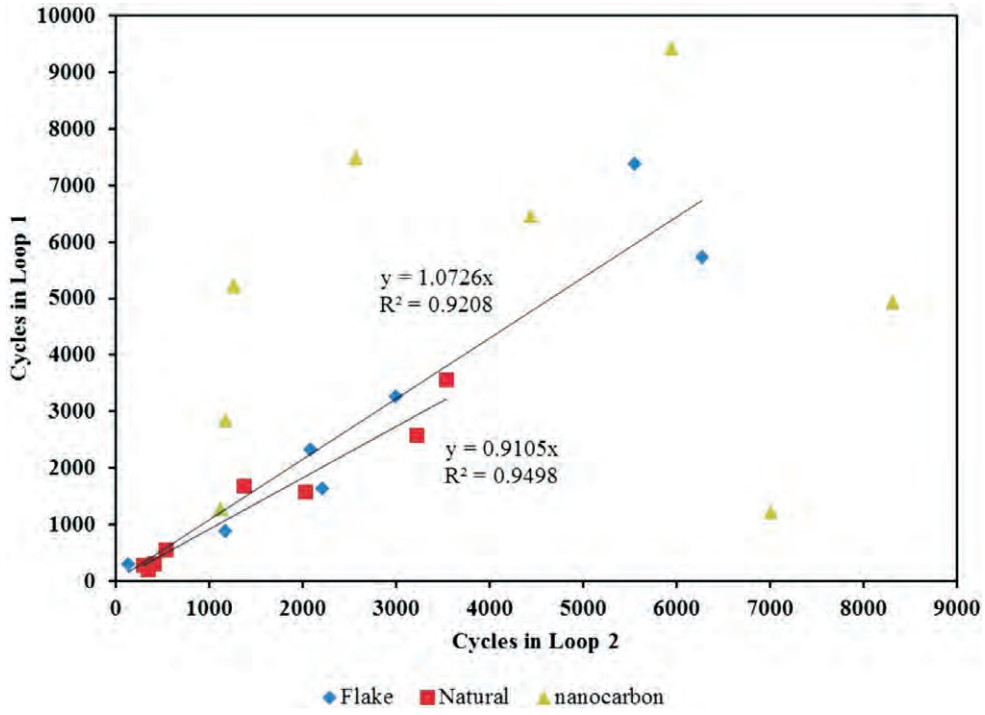

Figure 8 Correlation between the number of capacity cycles achieved in the first and second loop sequences of the HRPSoC analysis.

that, on average, the cells achieved a similar number of cycles between the first and second loop sequences. However, the comparison between the number of cycles in the first and second loops for the cells made with the nanocarbon showed no correlation; even though some cells that contained the nanocarbon showed a significant number of cycles more than similar cells made with the other graphites (Fig. 8).

Since this was not a notable trend across the cells studied, the improvement was not observed in the complete set of cells studied; and this finding will have to be verified by repeating the experiment for cells with similar formulations in the negative paste mixture, considering that there could be other factors that might contribute to the increase in capacity cycles within a loop sequence.

The variation of the paste density made with different added carbon amounts (Table 4) can be compared with the different discharge rates (C_1, C_{20} and CCA) in terms of their percentage material utilization (Fig. 9). The actual capacity (Ah) of a cell made with different electrodes that had different paste densities did vary from cell to cell. However, if the available material utilization was considered in a particular built cell, where the negative active material was the limiting component, no significant differences could be observed between the cells with varying paste densities.

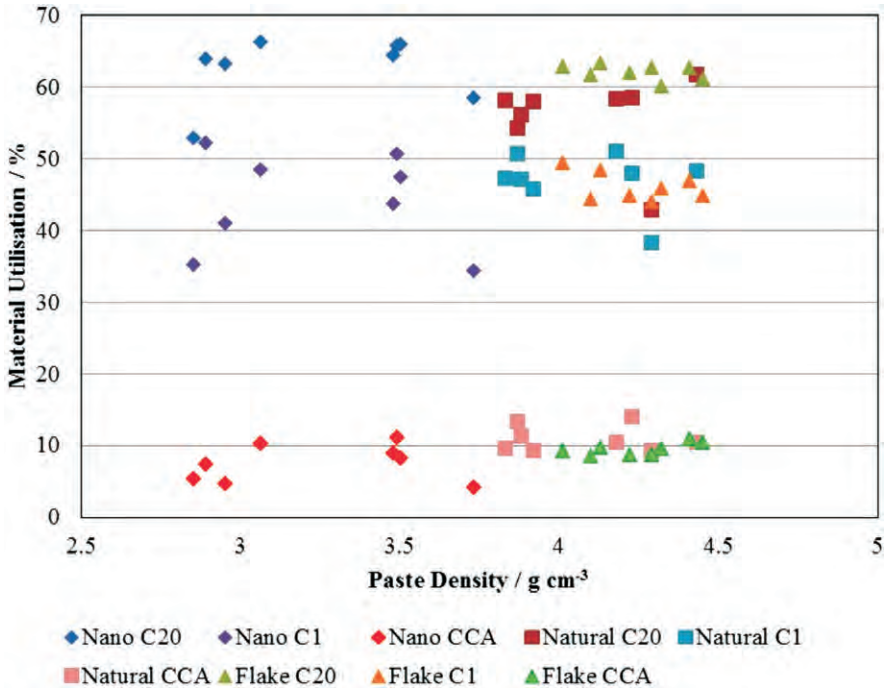

Figure 9 Variation in the percentage material utilization at different discharge capacities,based on the active material on the negative plates with respect to the variation in paste density for the cell types containing various added carbons.

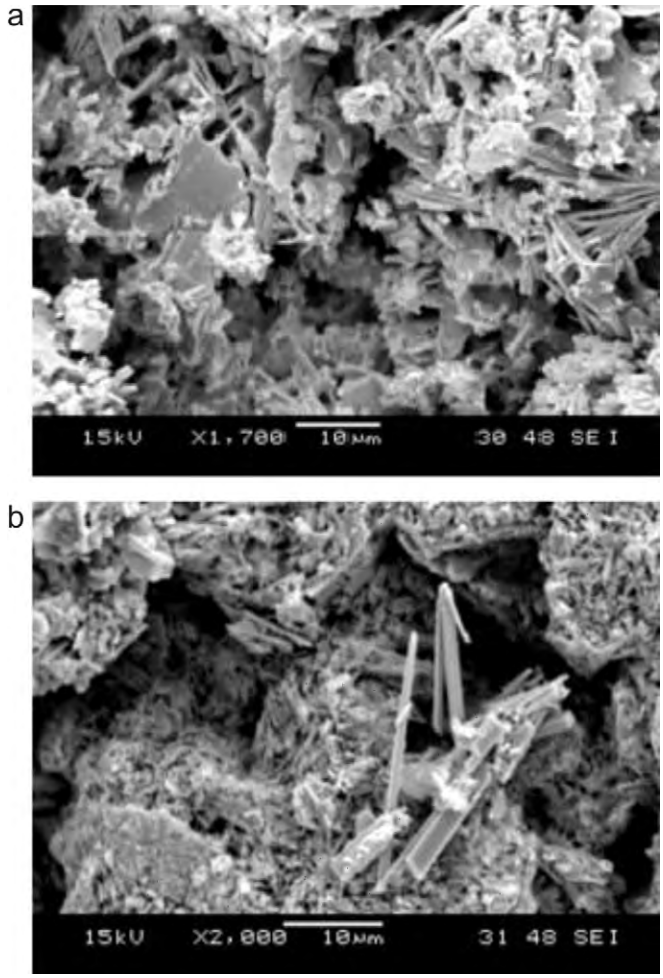

Figure 10 (**a**) SEM analysis of Pb active material containing natural graphite before capacity cycling; (**b**) SEM analysis of Pb active material containing natural graphite after capacity cycling.

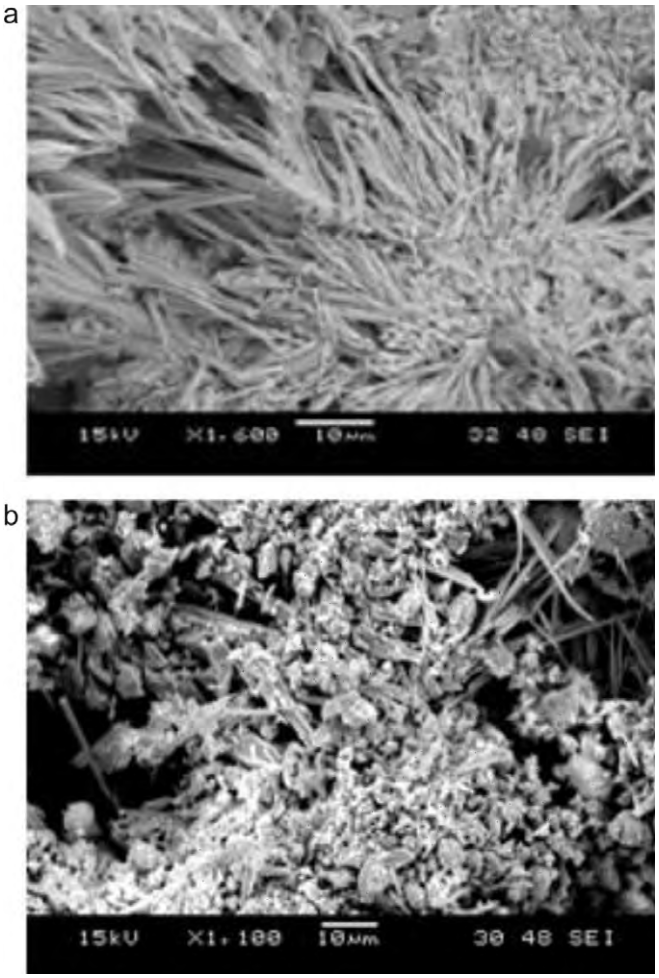

Figure 11 (**a**) SEM analysis of Pb-active material containing nanocarbon before capacity cycling; (**b**) SEM analysis of Pb active material containing nanocarbon after capacity cycling.

The results showed that the cells with the flake graphite achieved a workable paste with a density between 4.0 and 4.5 g cm^{-3}. These cells showed that there was very little variation in their achievable discharge material utilization at the different rates. For the cells made with natural graphite, the paste density varied between 3.8 and 4.5 g cm^{-3} and showed a slight variation in the respective material utilization capacity, but with no clear or significant correlation.

However, for the cells made with the nanocarbon, the paste density had to be significantly lowered and varied between 2.8 to 3.7 g cm^{-3}. The lower paste density was necessary for some of the samples, in order to allow for a workable paste. The high torque mixer was limited to the amount of strain the motor could apply; and the paste's rheology had to be adjusted by the addition of water, in order to allow for the material to mix effectively, and to allow for its pasting onto the grids by hand and roller.

A stiff paste gave a significant variation in the ability of the paste to be evenly distributed across the plate surface. Over the range of paste densities, the results showed significant variation in the material utilization capacity at the different rates – but with no clear correlation. This would support the fact that the paste densities should be controlled within a tightly controlled range, and that the variation in capacity utilization could be due to many other factors that were not investigated in this study.

The study did show, however, that a workable paste mixture with slight variation in paste density can achieve similar capacities in terms of the active material utilized. However, large variations in material-utilization capacity occur when the paste density becomes too low, and when the workability of the material is not consistent.

3.3. Electrode-active Material Characterization after HRPSoC

The cells that were subjected to HRPSoC were disassembled after cycle failure and analyzed for their failure mode by PXRD and SEM. The PXRD of the negative plate showed a significant amount of $PbSO_4$ that varied between 60 % and 80 % for the cells studied. The SEM images of the electrode material before and after capacity cycling showed that the large $PbSO_4$ observed after cycling was the main reason for the cell's failure (Figs 10 and 11).

The SEM images of the negative plate active material containing the natural graphite after formation show typical platelike crystals of Pb (Fig. 10a). The SEM images of the Pb with natural graphite after HRPSoC showed the breakdown of the Pb plate-like structures, with a large amount of needle-shaped crystals that are typical of $PbSO_4$ (Fig. 10b).

This type of crystal morphology was typical for the other formed and capacity cycled active material containing flake and natural graphite samples.

The formed active material made with nanocarbon showed a

slightly different morphology (Fig. 11a). The Pb crystals were more needle-shaped conglomerating around central nucleation points. The SEM images of the samples containing the nanocarbon after HRPSoC contained much finer $PbSO_4$ crystallites interspersed in the longer needle-shaped crystals(Fig. 11b).

4. Conclusion

The study showed that the use of DoE was a useful approach for looking at the effect of varying the amounts of additives to plate materials in batteries on a range of electrochemical properties (responses). A two-factorial design of low and high values of certain additives was shown to be a good way to evaluate how they would influence certain electrochemical parameters, and that further improvements in the design can be done by focussing on the additives that showed significant interactions and effects to the desired responses. It helps to eliminate any 'preconceived notions' that by increasing the amounts of certain additives, there will necessarily be an improvement.

The study showed that the amounts of the variables, Vanisperse and $BaSO_4$, and their interaction had a significant influence on responses, such as the Peukert constant (n), CCA discharge time and the ability to capacity cycle under partial state of charge for some of the types of graphites that were added to the negative paste mixture. Little or no effect in varying the amounts of the three types of added carbons added to the particular responses was observed. However, it was still important for the graphites to be in the paste mixture in small amounts.

The adapted HRPSoC method was shown to be suitable to subject a Pb-acid cell to a relatively quick comparative test (3–5 weeks) of continuous capacity cycling with multiple-loop sequences. The addition of small amounts of nanocarbon to the paste mixture was shown to change the negative active material's crystal morphology. There was only a slight improvement in partial state of capacity cycling in some cells made with the nanocarbon, and duplicate cells would have to be made to confirm these results.

Acknowledgements

The authors thank Willard Batteries for providing financial assistance, and for the various manufactured components used in the study. The authors thank the South African National Research Foundation (NRF) for their financial contribution. The authors thank Coos Bosma, from Innoventon, for helping with the statistical analysis of the results.

References

1 J. Valenciano, A. S'anchez, F. Trinidad and A.F. Hollenkamp, *J. Power Sources,* 2006, **158**, 851–863.
2 R. Wagner, M. Schroeder, T. Stephanblome and E. Handschin, *J. Power Sources,*1999, **78**(1–2), 156–163.
3 P.T. Moseley, *J. Power Sources*, 2004, **127**, 27–32.
4 M. Calabek, K. Micka, P. Krivak and P. Baca, *J. Power Sources*, 2006, **158**, 864–867.
5 D.P. Boden, D.V. Loosemore, M.A. Spence and T.D. Wojcinski, *J. Power Sources*, 2010, **195**, 4470–4493.
6 H. Vermesan, N. Hirai, M. Shiota and T. Tanaka, *J. Power Sources,* 2004, **133**, 52–58.
7 S. Osumi, M. Shiomi, K. Nakamura, K. Sawai, T. Funato, M. Watanabe and H. Wada, ALABC Project N5.2, August 2005.
8 A.F. Hollenkamp, W.G.A. Baldsing, S. Lau, O.V. Lim, R.H. Newnham, D.A.J. Rand, J.M. Rasalie, D.G. Vella and L.H. Vu, ALABC Project N1.2, Annual Report, July 2000 – June 2001.
9 M.A. Spence, D.P. Boden and T.D. Wojcinski, ALABC Project C1.1/2.1A. October 2009.
10 J. Anthony, *Design of Experiments for Engineers and Scientists*, Elsevier Science, Oxford, UK, 2003.
11 D. Doerffel and S.Abu Sharkh, *J. Power Sources,* 2006, **155**, 395–400.
12 D. Pavlov, P. Nikolov and Rogachev, T. *J. Power Sources*, 2010, **195**, 4435–4443.